Environmental Nanotechnology, Monitoring & Management 14 (2020) 100390

Contents lists available at ScienceDirect

Environmental Nanotechnology, Monitoring & Management

journal homepage: www.elsevier.com/locate/enmm

Punica granatum L. mesocarp-assisted rapid fabrication of gold nanoparticles and characterization of nano-crystals

Ghassan Adnan Naeem [a], Rasim Farraj Muslim [b], Muwafaq Ayesh Rabeea [c], Mustafa Nadhim Owaid [b,d,*], Nabeel Mohammed Abd-Alghafour [a,d]

[a] Department of Biophysics, College of Applied Sciences-Hit, University Of Anbar, Hit, Anbar 31007, Iraq
[b] Department of Environmental Sciences, College of Applied Sciences-Hit, University Of Anbar, Hit, Anbar 31007, Iraq
[c] Department of Applied Chemistry, College of Applied Sciences-Hit, University Of Anbar, Hit, Anbar 31007, Iraq
[d] Department of Heet Education, General Directorate of Education in Anbar, Ministry of Education, Hit, Anbar 31007, Iraq

ARTICLE INFO

Keywords:
Biomaterials
AuNPs
Pulp
Phytosynthesis of nanoparticles
Pomegranate

ABSTRACT

The preparation approaches of nanomaterials using organic residuals seek to strengthen the sustainable environment in the field of so-called Green Synthesis. The current study provides the experimental evaluation of residuals of the fleshy pulp (mesocarp) of pomegranate (*Punica granatum* L.) as a new reducing agent for AuNPs fabrication. This process took just 10 min to form AuNPs, and the reaction has included 25 μL of the pomegranate mesocarp extract with 50 mL Chloroauric acid (0.1 mM). The visual change in color, UV–vis spectroscopy, Zetasizer, Zeta Potential, FE-SEM, XRD, EDX, and FTIR were used to investigate AuNPs. These analyses have been demonstrated the generation of spherical AuNPs (18−30 nm) with high stability (−27.2 mV). The XRD pattern is crystalline and shows the Bragg peaks indicating the face-centered cubic (FCC) structure attributed to gold nanostructures (26.59 nm). FTIR revealed that the reducing agent formed from phenolic acids, flavonoids, tannins and anthocyanins, amino acids, and polysaccharides. The fabricated AuNPs by this green approach are useful and cheap at the commercial level to apply as a method remarkable in nanomedicine sciences in the future.

1. Introduction

The modern technology facilitated that huge amounts of materials such as carbon, wires, fibers, and rods were synthesized in the nanoscale range. The researches in nanomaterials associated with tiny things showed numerous applications in numerous scientific fields like biological, physical, chemistry, and materials sciences (Madhusudhan et al., 2014; Murray, 2008; Owaid, 2019; Sardar et al., 2009). These NPs can control single atoms that formed molecules. Nanotechnologies have a large potential to give technological explanations for various issues in science and medical fields (Aravind et al., 2013; Farkas et al., 2010). Nanomaterials as suspension particles with averaged size below 100 nm were prepared by green methods in addition to the chemical approach. Plants (Al-Bahrani et al., 2018; Muslim and Owaid, 2019) and fungi (Jaloot et al., 2020; Owaid et al., 2019; Rabeea et al., 2020) extracts widely have been effectively used as a reducer agent to synthesize metallic nanoparticles.

The pomegranate (*Punica granatum* L.) fruits consist of the calyx, seeds, peel (rind) (exocarp), pulp, or albedo (mesocarp) and carpellary membranes (endocarp). *P. granatum* fruits have different phenolic compounds showed antioxidant (He et al., 2012) and anticancer activities (Sharrif and Hamed, 2012). However, the fleshy pulpy mesocarp is extensively used in folk medicine due to its aldehydes, alcohols, and terpenes compounds (Vázquez-Araújo et al., 2011). Also, mesocarp has some tannic and phenolic compounds like punicalagin, gallic acid, ellagic acid, p-coumaric acid and protocatechuic acid (Fischer et al., 2011) while the exocarp contains anthocyanin, catechins, punicalin, ellagic acid, (Ismail et al., 2012), caffeic acid, gallic acid, pelletierine alkaloids, ellagitannins, kaempferol, luteolin, quercetin (Sreekumar et al., 2014), hydroxybenzoic acids, punicalagin (Kazemi et al., 2016) tannin compounds (Saad et al., 2012), which exhibit antioxidant activity. For centuries, peels of this fruit have been used for the treatment and prevention of diabetes, diarrhea, dysentery, dental plaque, and as antimicrobial, anti-influenza, anticancer, anti-inflammatory, anti-allergic (Ismail et al., 2012) and antioxidant (Abid et al., 2017) agents and were used to stimulate osteoblastic differentiation and prevent the bone loss (Spilmont et al., 2015). Only a few studies have concentrated on the synthesis of some metallic NPs with assistance pomegranate peels. Peels

* Corresponding author at: Department of Environmental Sciences, College of Applied Sciences-Hit, University Of Anbar, Hit, Anbar 31007, Iraq.
E-mail address: mustafanowaid@uoanbar.edu.iq (M.N. Owaid).

https://doi.org/10.1016/j.enmm.2020.100390
Received 23 June 2020; Received in revised form 29 August 2020; Accepted 20 October 2020
Available online 23 October 2020

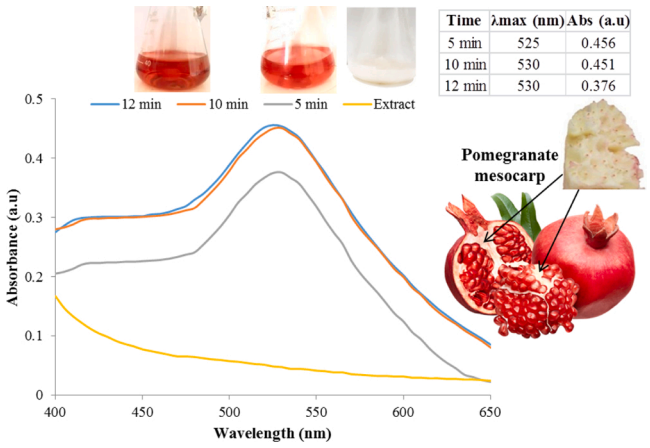

Fig. 1. UV–vis spectra of AuNPs and the mesocarp extract.

were used to synthesize AgNPs, which had antibacterial (Yang et al., 2016) and anticandidal efficacy (Fernandes et al., 2018) and AuNPs, which lead to killing Roundworms (Patel et al., 2019). Besides, proanthocyanidin isolated from Peels was used to synthesize AuNPs, which applied to decolorize Methylene blue dye (Biao et al., 2018).

To this time, there is no mention preparation of AuNPs using the aqueous pomegranate mesocarp extract (a pomegranate fruit residue). Therefore, this article has been focused on using small volume of the pomegranate mesocarp extract as an eco-friendly reducing agent to the rapid synthesis of AuNPs. This approach could be facilely commercialized for large amounts of production of AuNPs.

2. Materials and method

2.1. Chemicals

Chloroauric acid ($HAuCl_3.4H_2O$) was obtained from Direvo Industrial Biotechnology, Germany (purity, 99 %).

2.2. Samples of pomegranate fruits

The fruits of red pomegranate (*Punica granatum* L.) (Punicaceae) were collected from the local market of Hit city, Iraq. The pulp (mesocarp) of the fruits, which is considered a residual from consuming this fruit, was used to prepare the watery extract.

2.3. Preparation of the mesocarp extract

To prepare the mesocarp extract, the waste of pomegranate fruits was washed with deionized water. The mesocarp was collected and then cut into small pieces. The organic compounds in the fleshy mesocarp of pomegranate have been extracted using D.W at 70 °C (López Más et al., 2010) with stirring for 30 min. The extract was stored in the freeze at −20 °C.

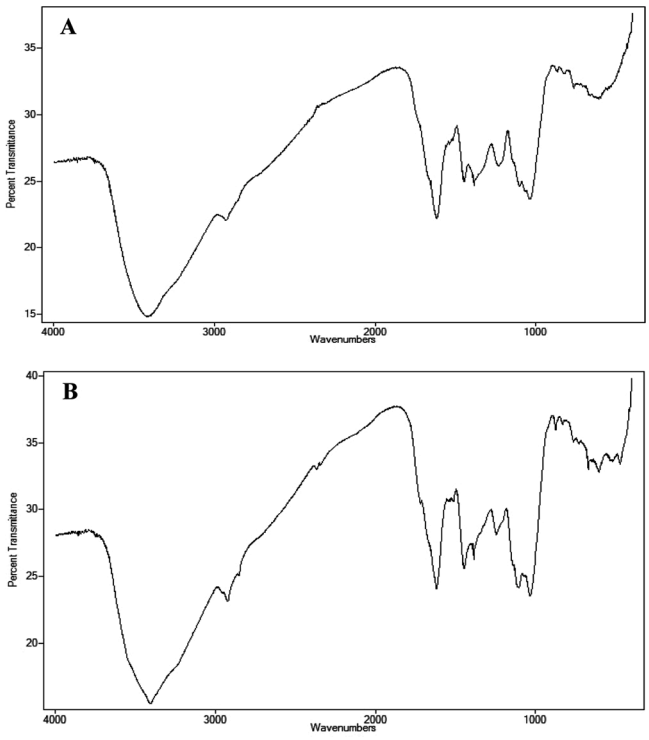

Fig. 2. FT-IR of the mesocarp extract (A) and AuNPs (B).

2.4. The green fabrication of Au nanoparticles

The gold NPs were achieved by adding 25 μL of the aqueous mesocarp extract on 50 mL trichloride hydrochloride (10^{-4} M) at 90 °C in Erlenmeyer flask-100 mL. The mixture color directly altered from colorless to light purple. Then after 5 min, the mixture became constant with the pink color, which indicated that the nucleation process finished.

2.5. Characterization of AuNPs

A UV–vis spectroscopy was used to observe the bioreduction agents of Au^+ ions to Au° atoms in the watery extract of mesocarp by the dual-beam spectrophotometer (Shimadzu, AV-1800) at range from 400−650 nm and to check the lambda max. FESEM (FESEM-FEI/Nova NanoSEM 450) (Field Emission Scanning Electron Microscopy) images confirmed the shape and size of mesocarp-AuNPs. The elemental composition of the sample was done using EDX (Energy Dispersive X-ray) analysis (Oxford-Instrument INCA400). The Zeta Potential value and hydrodynamic particle size of AuNPs were done using Zetasizer (Malvern Instruments Ltd., UK). The nondestructive technique XRD (X-

Table 1
Phytochemical analysis of the mesocarp by HPLC (Ambigaipalan et al., 2016).

Phenolic acids	Flavonoids	ellagic acid deoxyhexoside	tetragalloylglucopyranose
trans-*p*-coumaric acid	quercetin *3-O*-rhamnoside	ellagic acid hexoside	digalloyl-HHDP-glucoside (punigluconin)
vanillic acid	kaempferol *3-O*-glucoside	valoneic acid bilactone I, II	galloyl-bis-HHDP-hexoside (casuarinin)
gallic acid	*cis*-dihydrokaempferol hexoside	HHDP hexoside I, II	pentagalloylglucopyranose I
brevifolin carboxylic acid	*trans*-dihydrokaempferol hexoside	digalloyl hexoside	galloyl-HHDP-DHHDP-hex (granatin B)
coutaric acid	**Tannins**	punicalagin isomers	HHDP-gallagyl-hexoside I, II, III, IV (punicalagin)
p-hydroxybenzoic hexoside	ellagic acid	galloyl-HHDP-hexoside (corilagin)	**Anthocyanins**
vanillic acid hexoside	monogalloyl hexoside	trigalloylglucopyranose I	cyanidin-3-*O*-pentoside
caffeic acid hexoside	ellagic derivative, I, III	galloyl-HHDP-glucoside (lagerstannin C)	pelargonidin-3-*O*-glucoside
ferulic acid hexoside	ellagic acid pentoside	bis-HHDP-hexoside (pedunculagin I)	cyanidin-3-*O*-glucoside
5-O-caffeoylquinic acid	ellagic acid derivative	digalloyl-HHDP-gluc (pedunculagin II)	delphinidin-3-*O*-glucoside

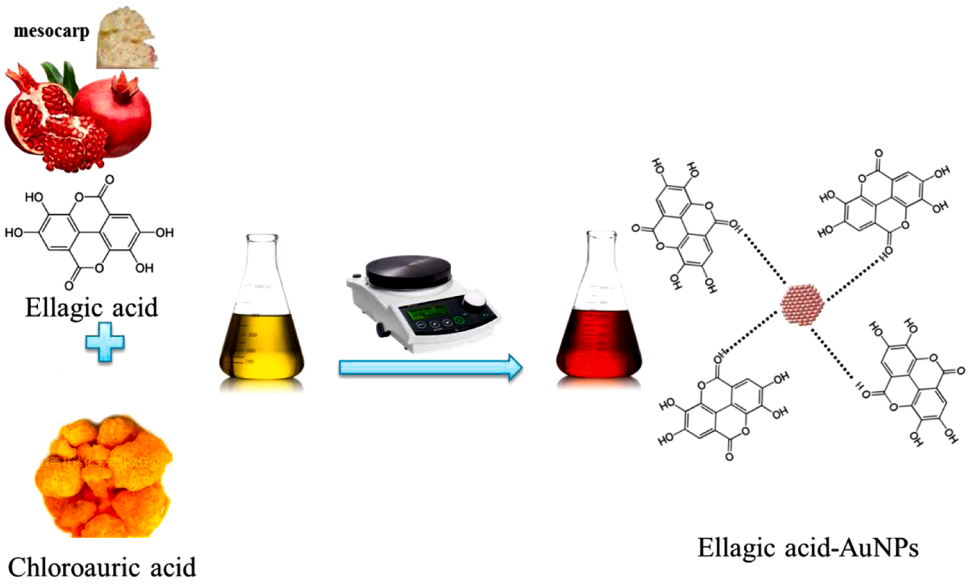

Fig. 3. The schematic chart of AuNP formation and the expected composition of ellagic acid (tannin) around atoms of gold.

Ray Diffraction) pattern confirmed the crystallinity of AuNPs by Bruker X-ray diffractometer (Shimadzu, Japan). The functional groups in the aqueous extract and the synthesized AuNPs were analyzed by FTIR (Fourier-Transform Infrared) Spectrometer (JASCO 4100).

3. Result and discussion

The current study includes eco-friendly synthesis of AuNPs from the fleshy pulp (mesocarp) of pomegranate as a new stabilizing and reducing agent. The phytosynthesis process steps started through observation of the color change in media (50 mL of 0.1 Mm AuNPs mixed with 25 μL of the aqueous mesocarp extract at 90 °C). Fig. 1 exhibited the kinetic schematic of the UV–vis of AuNPs and the aqueous extract. The spectrum line of UV–vis has recorded a lambda max at 520 nm. The color change in the aqueous solution from colorless to bright purple has been immediately exhibited with adding the first drop of the reducing agent, and then the color changed to pink after 5 min. The color intensified with advancing the reaction time that denoted AuNPs formed with more concentration after 5 min. The media color was constant on pink-red at the 8th min, due to the SPR (surface plasmon resonance) (Dheyab et al., 2020; Owaid et al., 2017) of Au°, indicated the formation and distribution of AuNPs uniformly. In addition, the remarkable intensity of AuNPs may be due to finding phenolic and polysaccharides components, which reduced and capped the formed NPs (Rabeea et al., 2020). The plot in Fig. 1 demonstrated that the increasing time to 12 min has no obvious impact on the SPR band and color of AuNPs compared to 10 min, so the optimum time is required to convert Au^{+} to Au° by the mesocarp extract is 10 min. The achieved results surpass the earlier works in this area (Biao et al., 2018; Patel et al., 2019) in terms of the maximum absorption peak of UV–vis. This is an

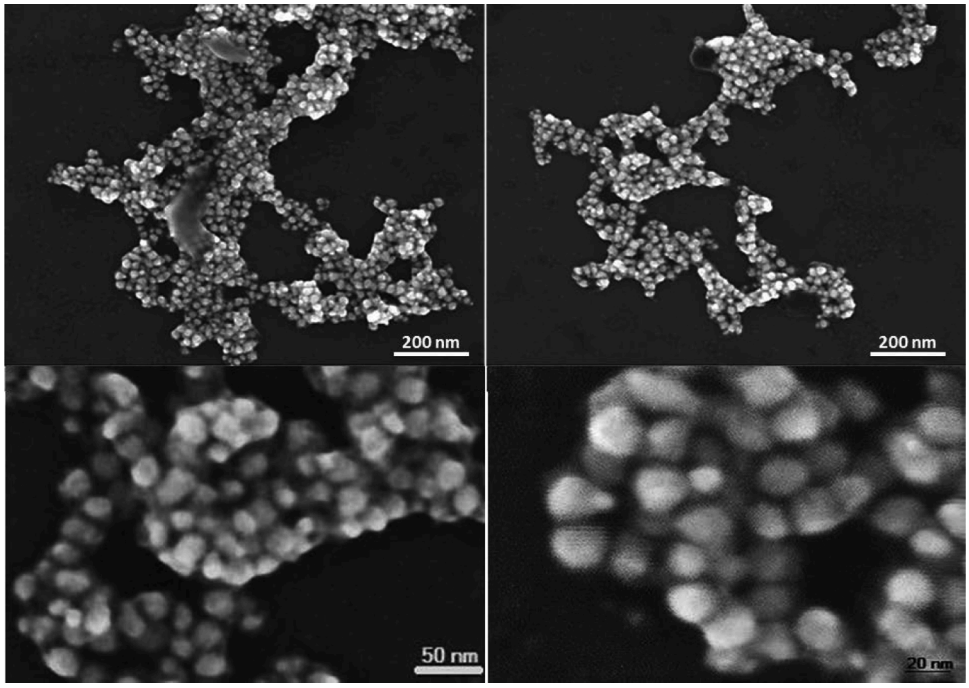

Fig. 4. FE-SEM images of the mesocarp-AuNPs.

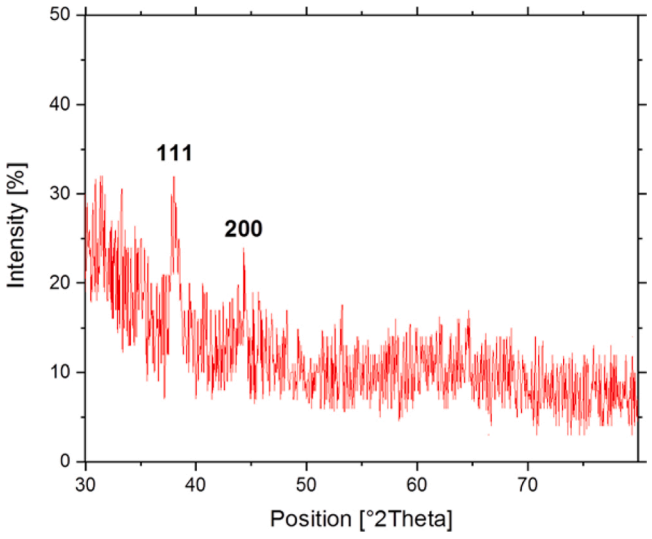

Fig. 5. XRD pattern of AuNPs biosynthesized using the aqueous extract of the pomegranate mesocarp.

interesting finding, and it could be hypothesized that the mesocarp is hopeful in the phyto-synthesizing AuNPs using the extract of plant residues.

The extract of the mesocarp was diagnosed using the infrared spectrum (FT-IR) to check the chemical components and the functional groups in their aqueous solution, as in Fig. 2. Also, it was applied to mesocarp-AuNPs. The similarity is observed in some bands' locations for the spectrum of the mesocarp extract and mesocarp-AuNPs. However, the spectrum of nanostructure has little differences in bands, especially in the region of functional groups such as hydroxyl of phenols and carboxylic acids. Fig. 2A exhibits two absorption bands at 1395 and 1425 cm^{-1}. While locations of these absorption bands in Fig. 2B shift at 1390 cm^{-1} and 1420 cm^{-1}. All of these bands are due to the aromatic ring vibrations. The set of absorption bands appears at 2865, 12,845, and 2920 cm^{-1} due to homogeneous stretch vibration of methyl and/or ethyl groups referees to the presence of the fatty acids in the mesocarp extract, while the heterogeneous stretch vibration band (2865 cm^{-1}) disappears in the mesocarp-AuNPs spectrum (Fig. 2B). Continuously, absorption bands at 1045 cm^{-1} and 1035 cm^{-1} belong to a single bond C—C in the extract and gold nanoparticles, respectively. Besides, the spectrum 2A shows the absorption band at 1710 cm^{-1} relates to the vibration of the carbonyl group (C═O) in mesocarp extract because of the finding of flavonoids and lipids. The other broad stretch vibrating band at 3390 cm^{-1} relates to the hydroxyl (−OH) groups, which imputes to phenolic compounds and lipids in the mesocarp composition. These two bands (C═O and −OH) shifted at 1700 cm^{-1} and 3400 cm^{-1} in mesocarp-AuNPs.

Many studies recorded active biological compounds in the mesocarp of pomegranate (Ambigaipalan et al., 2016; Campillo et al., 2015; Mena et al., 2012; Russo et al., 2020; Souleman and Ibrahim, 2016) as in Table 1. The mesocarp of pomegranate is rich with phenolic acids, tannins, flavonoids anthocyanins (Ambigaipalan et al., 2016), proteins (Miklavčič Višnjevec et al., 2017), and polysaccharides (Balli et al., 2020). Based on the orientations of its −OH and COOH groups in the FT-IR spectrum (Fig. 2), polyphenolic compounds relating to Ellagic acid have been proved. These types of bands (2800−3700 cm^{-1}) are compatible with the −OH band which is found on the benzene ring, and the band is broadly composed of a mixture of COOH and −OH groups on the ring. Additionally, the C═O stretching bands at 1710 cm^{-1} and the bands in the regions of 1000–1710 cm^{-1} obtained can belong to Ellagic acid in the mesocarp of pomegranate. Ellagic acid, found in the fruit of pomegranate, is composed from 4 phenolic groups, 4 lipophilic rings, and 2 lactones, which may play a significant role as an electron acceptor.

Table 2
The particles size and microstructral parameters of the synthesized Au nanoparticles.

d-spacing (Å)	Crystallite Size (D) (nm)	FWHM (β)	Dislocation density (δ) ($\times 10^{15}$ lines/m^2)	2θ	Planes
2.35751	11.73	0.7200	7.2678	38.14°	1 1 1
2.08473	41.45	0.2067	0.5820	43.40°	2 0 0

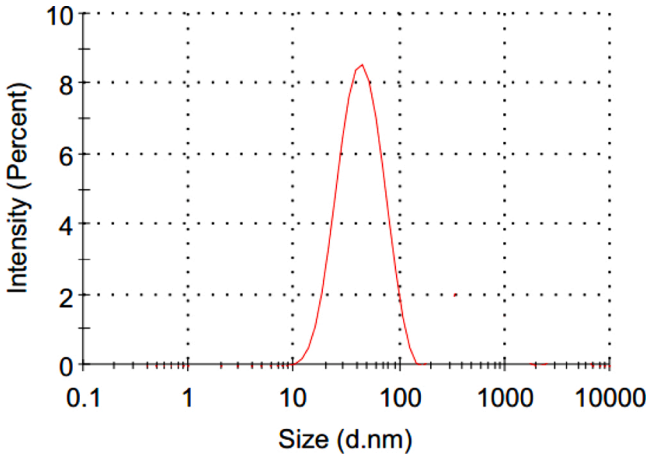

Fig. 6. Size distribution report of AuNPs by the intensity.

(Gumienna et al., 2016). The schematic chart of AuNP formation and expected composition of ellagic acid (tannin) of the gold atoms has been illustrated in Fig. 3.

The characterization of FESEM was performed to know the shape and size of AuNPs (Fig. 4). This figure displays FESEM images of the synthesized AuNPs with a magnification of 400 nm. The FESEM micrograph of AuNPs clearly shows that the average size of the nanoparticles at room temperature is around 18−30 nm, with various spherical shapes. The images show the embedding of spherical gold nanoparticles in the bio-matrix (Madhusudhan et al., 2014). Each spherical particle contains an even smaller aggregate of nanoparticles. The appearance of a few nanoparticles with a large size may be due to the agglomeration of gold nanoparticles (Farkas et al., 2010). This aggregation may be due to the decrease in the coating on the nuclei of the capping agent, which was developed at the later stage of nucleation and growth.

Fig. 5 showed the XRD pattern of AuNPs synthesized by an aqueous extract of the fleshy pulp (mesocarp) of pomegranate, indicates pure crystalline gold nature. The reflection peaks show the high purity of AuNPs, appeared at 38.14 and, 44.4 which correspond to (1 1 1), and (2 0 0), Miller indices, respectively.

The XRD pattern is crystalline and shows the Bragg peaks indicating the structure of FCC (face-centered cubic) attributed to the nanostructure of gold, which correlates well with the standard peaks from the data card 04-0784 (JCPDS) for the gold element. Two peaks are observed (1 1 1) and (2 0 0) planes. The characteristic of FCC structure and the broadening of peaks confirmed the phytosynthesizing AuNPs. The grain sizes (D) of the synthesized gold nanoparticles are 11.73, and 41.45 nm for (1 1 1) and (2 0 0) planes, respectively and the average size is 26.59 nm. Similar results were observed by Rajakumar et al. (Rajakumar et al., 2016), who found that the average nanoparticle size of phytosynthesized gold nanoparticles was 28 nm. The Debye-Scherrer Eq. (1) was employed to evaluate the average nanoparticle size (Owaid et al., 2020) :

$$D = \frac{k\lambda}{\beta \cos\theta} \quad (1)$$

Table 3
Comparison of the synthesis of metallic NPs from pomegranate fruits with the previously published related literature.

The used part as a reducing agent	Metallic NPs Type	Sizes of NPs	Shapes of NPs	Crystallized nature and planes peaks	Conditions (temperature and time of reaction)	Ratio of extract:salt	References
Peels	AgNPs	15−35 nm	spherical	five crystal faces (1 1 1), (2 0 0), (2 2 0), (3 1 1), (2 2 2)	35 °C (1 h)	50 mL + 100 mL (5 mM, $AgNO_3$)	(Yang et al., 2016)
Peels	AgNPs	89 nm	various	face centered cubic (1 1 1), (2 0 0), (2 2 0), (3 1 1), (2 2 2)	50 °C (12 min)	30 mg/mL +(100 mM $AgNO_3$)	(Fernandes et al., 2018)
Peels	AuNPs	11 nm	round	ND	25 °C (24 h)	900 µl + 25 mL (1 mM, $HAuCl_3.4H_2O$)	(Patel et al., 2019)
Proanthocyanidin isolated from Peels	AuNPs	14.5 nm	spherical	face centered cubic (1 1 1), (2 0 0), (2 2 0), (3 1 1)	140 °C (4 h)	50 mL of 0.64 mM +0.64 mL (2 %, $HAuCl_3.4H_2O$)	(Biao et al., 2018)
Mesocarp	AuNPs	18−30 nm	spherical	face-centered cubic (1 1 1), (2 0 0)	90 °C (10 min)	25 µL + 50 mL (0.1 mM, $HAuCl_3.4H_2O$)	This study

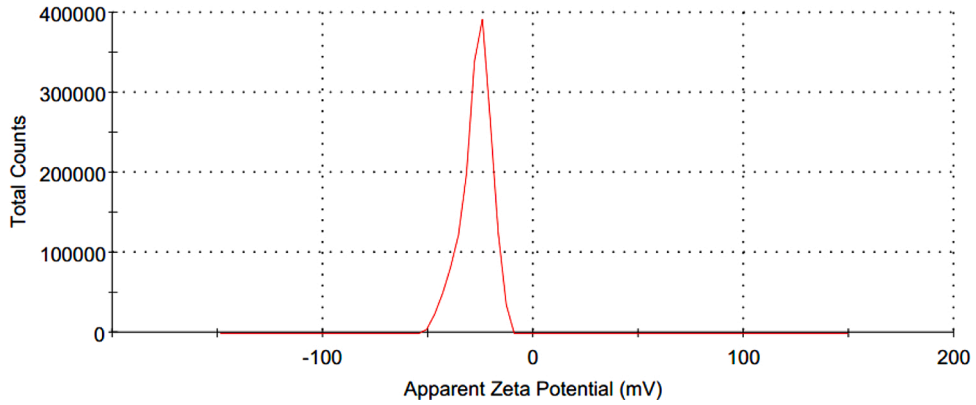

Fig. 7. The Zeta potential image (mV) of AuNPs.

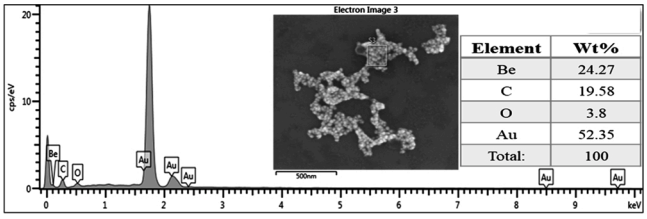

Fig. 8. EDX of the phytosynthesized AuNPs using the mesocarp extract.

where 'D' is particle diameter size, λ (Lambda) is the X-ray wavelength used (0.15406 nm), K is a constant approximately equal to 0.89, θ is the Bragg angle for the diffraction, β is the Full Width Half Maximum (FWHM) values converted from (degree) to the radial angle after multiplying it by $\left(\frac{\pi}{180}\right)$. The particle sizes and microstructural parameters of the mesocarp-AuNPs are recorded in Table 2. While the dislocation density (δ) was calculated by Eq. (2) (Abdul-Hadi et al., 2020):

$$\delta = (1/D^2) \quad (2)$$

Fig. 6 displays the particle size distribution measurements for the synthesizing smallest Au nanoparticles. This study was done with Zeta sizer, which gave a distribution of the particle size. Zeta potential was calculated in the same way for Au nanoparticles. The distribution of the particle size by intensity was found to change from 21 nm to 911 nm. The peak amplitude, peak area, and peak number provide significant interpretations for the nanoparticles in size and size distribution. When there is one peak, Zeta sizer shows a real particle size average. If there is more than one peak at Zeta sizer distribution, the particle size should be considered for the measurements.

In this study, the sizes 18−30 nm of AuNPswere synthesized from the mesocarp for the first time by using a small volume of the extract (only 25 µL) with a very low concentration of the gold salt (0.1 mM) during just 10 min. The planes of crystal were face-centered cubic (1 1 1) and (2 0 0), which showed controlling on the shapes and sizes of NPs as in XRD and FE-SEM (Figs. 4 and 5). Only a few studies have concentrated on the synthesis of some metallic NPs with assistance pomegranate peels like AgNPs (Fernandes et al., 2018; Yang et al., 2016) and AuNPs (Biao et al., 2018; Patel et al., 2019). The previous studies showed different measurements, as in Table 3.

The negative charge of the Zeta potential was also another significant measure of particle size (Murray, 2008). Zeta potential calculations were negative at the end of the reduction reaction due to resulting ions. Hence, this study obtained the diameters of nanoparticles smaller than 100 nm. In the framework of this analysis, the zeta potential of the synthesized AuNPs was obtained of -27.2 mV. The findings were also consistent with the literature results (Sardar et al., 2009).

The zeta potential value calculation has checked the stability of phytosynthesized AuNPs (Fig. 7). However, it revealed surface zeta potential, which showed the AuNPs surface charge. Besides, this analysis showed the constancy of the mesocarp-AuNPs (Srikar et al., 2016). Therefore, the mesocarp-AuNPs exhibited a remarkable zeta potential value reached -27.2 ± 7.27 mV (decent value) with the aggregation of AuNPs. Besides, the negative value of this analysis suggested that the gold NP is surrounded by some bioorganic molecules found in the mesocarp extract with a negative charge, which decreases the mesocarp-AuNPs repulsion and therefore rise the stability (Suresh et al., 2011). However, many studies reported how the stabilizers (surface-active molecules) formed electrostatic interactions in the reaction mixture yield more stable gold nanoparticles (Ahmad et al., 2015; Anand et al., 2015). It is proposed that organic compounds/molecules of

mesocarp, including phenols, flavonoids, tannins, and anthocyanins (Ambigaipalan et al., 2016), proteins (Miklavčič Višnjevec et al., 2017), and polysaccharides (Balli et al., 2020) can act as stabilizers in charge of phytosynthesis and stabilization of gold NPs.

EDX spectroscopy confirmed the AuNPs formation (Fig. 8). It indicates a high peak energy signal between 1 and 2 keV. The presence of elemental compounds oxygen, and carbon, along with gold, was also observed in the EDX graph because of the organic materials of mesocarp. In contrast, the beryllium element was observed due to the detector of EDS that uses a beryllium film (thickness, 8−10 μm) as a window material for maintaining the vacuum of the semiconductor detector. Beryllium window EDS detector leads to observe the Be signals in the EDX pattern (Liao, 2018).

4. Conclusion

In this study, the produced waste from consuming pomegranate (mesocarp) as a non-toxic surplus substrate is available, eco-friendly, and very efficient without using any capping agent to synthesize mesocarp-AuNPs. This approach demonstrated that the physicochemical properties of biosynthesized AuNPs were enhanced by using the mesocarp of pomegranate (*Punica granatum* L.). Applicable analyses have been shown the fabrication of 18−30 nm AuNPs (spherical) by FESEM images with high stability about −27.2 mV by the value of Zeta Potential. The XRD pattern showed a crystalline nature and face-centered cubic structure attributed to gold nanostructures with a size of 26.59 nm. FTIR indicated that the reducing agent formed from phenolic acids, flavonoids, tannins and anthocyanins, amino acids, and polysaccharides. The fabricated AuNPs by this green approach are useful and cheap at the commercial level to apply as a method remarkable in various filed.

Authorship statement

M A Rabeea, G A Naeem: substantial contribution to conception and design.

M N Owaid, M A Rabeea: substantial contribution to acquisition of data.

R F Muslim, G A Naeem: substantial contribution to analysis and interpretation of data.

M N Owaid, R F Muslim: drafting the article.

M A Rabeea, N M Abd-Alghafour: critically revising the article for important intellectual content.

M N Owaid, M A Rabeea: final approval of the version to be published.

Declaration of Competing Interest

The authors report no declarations of interest.

Acknowledgments

The author and co-authors thank the staff of College of Applied Sciences-Hit at University Of Anbar to complete the research project No. 3/92 on 13 October 2019.

References

Abdul-Hadi, S.Y., Owaid, M.N., Rabeea, M.A., Abdul Aziz, A., Jameel, M.S., 2020. Rapid mycosynthesis and characterization of phenols-capped crystal gold nanoparticles from Ganoderma applanatum, Ganodermataceae. Biocatal. Agric. Biotechnol. 27, 101683 https://doi.org/10.1016/j.bcab.2020.101683.

Abid, M., Yaich, H., Cheikhrouhou, S., Khemakhem, I., Bouaziz, M., Attia, H., Ayadi, M. A., 2017. Antioxidant properties and phenolic profile characterization by LC–MS/MS of selected Tunisian pomegranate peels. J. Food Sci. Technol. 54, 2890–2901. https://doi.org/10.1007/s13197-017-2727-0.

Ahmad, A., Wei, Y., Syed, F., Imran, M., Khan, Z.U.H., Tahir, K., Khan, A.U., Raza, M., Khan, Q., Yuan, Q., 2015. Size dependent catalytic activities of green synthesized gold nanoparticles and electro-catalytic oxidation of catechol on gold nanoparticles modified electrode. RSC Adv. 5, 99364–99377.

Al-Bahrani, R.M., Muayad, S., Majeed, A., Owaid, M.N., 2018. Phyto-fabrication, characteristics and anti-candidal effects of silver nanoparticles from leaves of Ziziphus mauritiana Lam. Acta Pharm. Sci. 56, 85–92. https://doi.org/10.23893/1307-2080.APS.05620.

Ambigaipalan, P., De Camargo, A.C., Shahidi, F., 2016. Phenolic compounds of pomegranate byproducts (Outer skin, Mesocarp, divider membrane) and their antioxidant activities. J. Agric. Food Chem. 64, 6584–6604. https://doi.org/10.1021/acs.jafc.6b02950.

Anand, K., Gengan, R.M., Phulukdaree, A., Chuturgoon, A., 2015. Agroforestry waste moringa oleifera petals mediated green synthesis of gold nanoparticles and their anti-cancer and catalytic activity. J. Ind. Eng. Chem. 21, 1105–1111. https://doi.org/10.1016/j.jiec.2014.05.021.

Aravind, G., Debjit, B., Duraivel, S., Harish, G., 2013. Traditional and medicinal uses of Carica papaya. J. Med. Plants Stud. 1, 7–15.

Balli, D., Cecchi, L., Khatib, M., Bellumori, M., Cairone, F., Carradori, S., Zengin, G., Cesa, S., Innocenti, M., Mulinacci, N., 2020. Characterization of arils juice and peel decoction of fifteen varieties of punica Granatum L.: a focus on anthocyanins, ellagitannins and polysaccharides. Antioxidants 9, 1–20. https://doi.org/10.3390/antiox9030238.

Biao, L., Tan, S., Meng, Q., Gao, J., Zhang, X., Liu, Z., Fu, Y., 2018. Green synthesis, characterization and application of proanthocyanidins-functionalized gold nanoparticles. Nanomaterials 8, 53. https://doi.org/10.3390/nano8010053.

Campillo, N., Viñas, P., Férez-Melgarejo, G., Ochotorena, M.L., Hernández-Córdoba, M., 2015. Determination of phenolic acids and hydrolyzable tannins in pomegranate fruit and beverages by liquid chromatography with diode array detection and time-of-Flight mass spectrometry. Food Anal. Methods 8, 1315–1325. https://doi.org/10.1007/s12161-014-0013-6.

Dheyab, M., Owaid, M., Rabeea, M., Aziz, A., Jameel, M., 2020. Mycosynthesis of gold nanoparticles by the Portabello mushroom extract, Agaricaceae, and their efficacy for decolorization of Azo dye. Environ. Nanotechnol. Monit. Manag. 100312. https://doi.org/10.1016/j.enmm.2020.100312.

Farkas, J., Christian, P., Urrea, J.A., Roos, N., vd Hassello, M., Tollefsen, K.E., 2010. Effects of silver and gold nanoparticles on rainbow trout (Oncorhynchus mykiss) hepatocytes. Aquat. Toxicol. 96, 44–52.

Fernandes, R.A., Berretta, A.A., Torres, E.C., Buszinski, A.F.M., Fernandes, G.L., Mendes-Gouvêa, C.C., De Souza-Neto, F.N., Gorup, L.F., De Camargo, E.R., Barbosa, D.B., 2018. Antimicrobial potential and cytotoxicity of silver nanoparticles phytosynthesized by pomegranate peel extract. Antibiotics 7, 1–14. https://doi.org/10.3390/antibiotics7030051.

Fischer, U.A., Carle, R., Kammerer, D.R., 2011. Identification and quantification of phenolic compounds from pomegranate (Punica granatum L.) peel, mesocarp, aril and differently produced juices by HPLC-DAD-ESI/MSn. Food Chem. 127, 807–821. https://doi.org/10.1016/j.foodchem.2010.12.156.

Gumienna, M., Szwengiel, A., Górna, B., 2016. Bioactive components of pomegranate fruit and their transformation by fermentation processes. Eur. Food Res. Technol. 242, 631–640. https://doi.org/10.1007/s00217-015-2582-z.

He, L., Zhang, X., Xu, H., Xu, C., Yuan, F., Knez, Ž., Novak, Z., Gao, Y., 2012. Subcritical water extraction of phenolic compounds from pomegranate (Punica granatum L.) seed residues and investigation into their antioxidant activities with HPLC-ABTS + assay. Food Bioprod. Process. 90, 215–223. https://doi.org/10.1016/j.fbp.2011.03.003.

Ismail, T., Sestili, P., Akhtar, S., 2012. Pomegranate peel and fruit extracts: a review of potential anti-inflammatory and anti-infective effects. J. Ethnopharmacol. 143, 397–405. https://doi.org/10.1016/j.jep.2012.07.004.

Jaloot, A.S., Owaid, M.N., Naeem, G.A., Muslim, R.F., 2020. Mycosynthesizing and characterizing silver nanoparticles from the mushroom Inonotus hispidus (Hymenochaetaceae), and their antibacterial and antifungal activities. Environ. Nanotechnol. Monit. Manag. 14, 100313 https://doi.org/10.1016/j.enmm.2020.100313.

Kazemi, M., Karim, R., Mirhosseini, H., Abdul Hamid, A., 2016. Optimization of pulsed ultrasound-assisted technique for extraction of phenolics from pomegranate peel of Malas variety: punicalagin and hydroxybenzoic acids. Food Chem. 206, 156–166. https://doi.org/10.1016/j.foodchem.2016.03.017.

Liao, Y., 2018. Practical Electron Microscopy and Database, 2nd ed.

López Más, J.A., Streitenberger, S.A., Peñalver Mellado, M., Martínez Ortis, P., 2010. Process for Preparing Pomegranate Extracts. Eur Pat Specif. EP1967079B1 European Patent Specification.

Madhusudhan, A., Reddy, G.B., Venkatesham, M., Veerabhadram, G., 2014. Efficient pH dependent drug delivery to target Cancer cells by gold nanoparticles capped with carboxymethyl chitosan. Int. J. Mol. Sci. 15, 8216–8234.

Mena, P., Calani, L., Dall'Asta, C., Galaverna, G., García-Viguera, C., Bruni, R., Crozier, A., Del Rio, D., 2012. Rapid and comprehensive evaluation of (Poly) phenolic compounds in pomegranate (Punica granatum L.) Juice by UHPLC-MSn. Molecules 17, 14821–14840. https://doi.org/10.3390/molecules171214821.

Miklavčič Višnjevec, A., Ota, A., Skrt, M., Butinar, B., Smole Možina, S., Gunde Cimerman, N., Nečemer, M., Baruca Arbeiter, A., Hladnik, M., Krapac, M., Ban, D., Bučar-Miklavčič, M., Poklar Ulrih, N., Bandelj, D., 2017. The genetic, biochemical, nutritional and antimicrobial characteristics of pomegranate (Punica granatum L.) grown in Istria. Food Technol. Biotechnol. 55, 151–163. https://doi.org/10.17113/ftb.55.02.17.4786.

Murray, R.W., 2008. Nanoelectrochemistry: metal nanoparticles, nanoelectrodes, and nanopores. Chem. Rev. 108, 2688–2720.

Muslim, R.F., Owaid, M.N., 2019. Synthesis, characterization and evaluation of the anti-cancer activity of silver nanoparticles by natural organic compounds extracted from

Cyperus sp. rhizomes. Acta Pharm. Sci. 57, 129–146. https://doi.org/10.23893/1307-2080.aps.05708.
Owaid, M.N., 2019. Green synthesis of silver nanoparticles by Pleurotus (oyster mushroom) and their bioactivity : review. Environ. Nanotechnol. Monit. Manag. 12, 100256 https://doi.org/10.1016/j.enmm.2019.100256.
Owaid, M.N., Al-Saeedi, S.S.S., Abed, I.A., 2017. Biosynthesis of gold nanoparticles using yellow oyster mushroom Pleurotus cornucopiae var. citrinopileatus. Environ. Nanotechnol. Monit. Manag. 8, 157–162. https://doi.org/10.1016/j.enmm.2017.07.004.
Owaid, M.N., Rabeea, M.A., Abdul Aziz, A., Jameel, M.S., Dheyab, M.A., 2019. Mushroom-assisted synthesis of triangle gold nanoparticles using the aqueous extract of fresh Lentinula edodes (shiitake), Omphalotaceae. Environ. Nanotechnol. Monit. Manag. 12, 100270 https://doi.org/10.1016/j.enmm.2019.100270.
Owaid, M.N., Naeem, G.A., Muslim, R.F., Oleiwi, R.S., 2020. Synthesis, characterization and antitumor efficacy of silver nanoparticle from Agaricus bisporus pileus, Basidiomycota. Walailak J. Sci. Technol. 17, 75–87.
Patel, M., Siddiqi, N.J., Sharma, P., Alhomida, A.S., Khan, H.A., 2019. Reproductive toxicity of pomegranate peel extract synthesized gold nanoparticles: a multigeneration study in C. elegans. J. Nanomater. 2019, 8767943. https://doi.org/10.1155/2019/8767943.
Rabeea, M.A., Owaid, M.N., Abdul Aziz, A., Jameel, M.S., Dheyab, M.A., 2020. Mycosynthesis of gold nanoparticles using the extract of Flammulina velutipes, Physalacriaceae, and their efficacy for decolorization of methylene blue. J. Environ. Chem. Eng. 8, 103841 https://doi.org/10.1016/j.jece.2020.103841.
Rajakumar, G., Gomathi, T., Rahuman, A.A., Thiruvengadam, M., Mydhili, G., Kim, S., Lee, T., Chung, I.-M., 2016. Applied sciences biosynthesis and biomedical applications of gold nanoparticles using Eclipta prostrata leaf extract. Appl. Sci. 6, 222. https://doi.org/10.3390/app6080222.
Russo, M., Cacciola, F., Arena, K., Mangraviti, D., de Gara, L., Dugo, P., Mondello, L., 2020. Characterization of the polyphenolic fraction of pomegranate samples by comprehensive two-dimensional liquid chromatography coupled to mass spectrometry detection. Nat. Prod. Res. 34, 39–45. https://doi.org/10.1080/14786419.2018.1561690.
Saad, H., Charrier-El Bouhtoury, F., Pizzi, A., Rode, K., Charrier, B., Ayed, N., 2012. Characterization of pomegranate peels tannin extractives. Ind. Crops Prod. 40, 239–246. https://doi.org/10.1016/j.indcrop.2012.02.038.
Sardar, R., Funston, A.M., Mulvaney, P., Murray, R.W., 2009. Gold nanoparticles: past, present, and future. Langmuir 25, 13840–13851. https://doi.org/10.1021/la9019475.
Sharrif, M.M., Hamed, H.K., 2012. Chemical composition of the plant Punica granatum L. (Pomegranate) and its effect on heart and cancer. J. Med. Plants Res. 6, 5306–5310. https://doi.org/10.5897/jmpr11.577.
Souleman, A.A., Ibrahim, G., 2016. Evaluation of Egyptian pomegranate cultivars for antioxidant activity, phenolic and flavonoid contents. Egypt Pharm. J. 15, 143. https://doi.org/10.4103/1687-4315.197582.
Spilmont, M., Léotoing, L., Davicco, M.J., Lebecque, P., Miot-Noirault, E., Pilet, P., Rios, L., Wittrant, Y., Coxam, V., 2015. Pomegranate peel extract prevents bone loss in a preclinical model of osteoporosis and stimulates osteoblastic differentiation in vitro. Nutrients 7, 9265–9284. https://doi.org/10.3390/nu7115465.
Sreekumar, S., Sithul, H., Muraleedharan, P., Azeez, J.M., Sreeharshan, S., 2014. Pomegranate fruit as a rich source of biologically active compounds. Biomed Res. Int. 2014, 686921. https://doi.org/10.1155/2014/686921.
Srikar, S.K., Giri, D.D., Pal, D.B., Mishra, P.K., Upadhyay, S.N., 2016. Green synthesis of silver nanoparticles: a review. Green Sustain. Chem. 6, 34–56. https://doi.org/10.4236/gsc.2016.61004.
Suresh, A.K., Doktycz, M.J., Wang, W., Moon, J.W., Gu, B., Meyer III, H.M., Hensley, D. K., Retterer, S.T., Allison, D.P., Phelps, T.J., 2011. Monodispersed Biocompatible Ag2S Nanoparticles: Facile Extracellular Bio-fabrication Using the Gamma-proteobacterium, S. Oneidensis. Oak Ridge National Laboratory (ORNL); Center for Nanophase Materials Sciences; High Temperature Materials Laboratory.
Vázquez-Araújo, L., Chambers, E., Adhikari, K., Carbonell-Barrachina, A.A., 2011. Physico-chemical and sensory properties of pomegranate juices with pomegranate albedo and carpellar membranes homogenate. LWT - Food Sci. Technol. 44, 2119–2125. https://doi.org/10.1016/j.lwt.2011.07.014.
Yang, H., Ren, Y., Wang, T., Wang, C., 2016. Preparation and antibacterial activities of Ag/Ag+/Ag3+ nanoparticle composites made by pomegranate (Punica granatum) rind extract. Results Phys. 6, 299–304. https://doi.org/10.1016/j.rinp.2016.05.012.